Increases in China's wind energy production from the recovery of wind speed since 2012

Yi Liu, Zhenzhong Zeng, Rongrong Xu, Alan D Ziegler, Sonia Jerez, Deliang Chen, Cesar Azorin-Molina, Lihong Zhou, Xinrong Yang, Haiwei Xu, et al.

ENVIRONMENTAL RESEARCH
LETTERS

LETTER • OPEN ACCESS

Increases in China's wind energy production from the recovery of wind speed since 2012

To cite this article: Yi Liu *et al* 2022 *Environ. Res. Lett.* **17** 114035

ENVIRONMENTAL RESEARCH
LETTERS

OPEN ACCESS

RECEIVED
19 July 2022

REVISED
21 September 2022

ACCEPTED FOR PUBLICATION
24 October 2022

PUBLISHED
4 November 2022

LETTER

Increases in China's wind energy production from the recovery of wind speed since 2012

Yi Liu[1], Zhenzhong Zeng[1,*], Rongrong Xu[1], Alan D Ziegler[2], Sonia Jerez[3], Deliang Chen[4], Cesar Azorin-Molina[5], Lihong Zhou[1], Xinrong Yang[1], Haiwei Xu[6], Laurent Li[7], Li Dong[8], Feng Zhou[9], Renjing Cao[10], Junguo Liu[1], Bin Ye[1], Xingxing Kuang[1] and Xin Yang[1]

[1] School of Environmental Science and Engineering, Southern University of Science and Technology, Shenzhen, People's Republic of China
[2] Faculty of Fisheries Technology and Aquatic Resources, Mae Jo University, Chiang Mai, Thailand
[3] Department of Physics, University of Murcia, 30100 Murcia, Spain
[4] Regional Climate Group, Department of Earth Sciences, University of Gothenburg, Gothenburg, Sweden
[5] Centro de Investigaciones sobre Desertificación, Consejo Superior de Investigaciones Científicas (CIDE, CSIC-UV-Generalitat Valenciana), Climate, Atmosphere and Ocean Laboratory (Climatoc-Lab), Moncada, Valencia, Spain
[6] College of Civil Engineering and Architecture, Zhejiang University, Hangzhou 310058, People's Republic of China
[7] Laboratoire de Météorologie Dynamique, Centre National de la Recherche Scientifique, Sorbonne Université, Ecole Normale Supérieure, Ecole Polytechnique, Paris, France
[8] Department of Earth and Space Science, Southern University of Science and Technology, Shenzhen, People's Republic of China
[9] Sino-French Institute for Earth System Science, College of Urban and Environmental Sciences, Peking University, Beijing, People's Republic of China
[10] Department of Mechanics and Aerospace Engineering, Southern University of Science and Technology, Shenzhen, People's Republic of China
[*] Author to whom any correspondence should be addressed.

E-mail: zengzz@sustech.edu.cn

Keywords: wind speed recovery, capacity factor, wind power gain, wind turbine selection, multiple scenarios

Supplementary material for this article is available online

Abstract

China has realized a 56-fold increase in installed wind capacity, from 5.9 GW in 2007 to 328 GW in 2021. In addition to increasing installed capacity, plans to substantially increase wind energy production for climate change mitigation also depend on future wind speeds, which strongly influences the efficiencies of installed turbines within individual wind farms. A reversal in globally decreasing wind speeds over several decades has been reported previously. However, subsequent studies using other data sources reported only a slight increase or no reversal in China. These uncertainties regarding China's wind energy production hamper estimates of wind energy production potential. Here, our analysis of quality-controlled wind speed measurements from *in-situ* stations shows that the wind speed decline in China reversed significantly since 2012 ($P < 0.001$), but with substantial spatio-temporal variability. We further estimated the capacity factor (CF) growth and the wind power gain solely associated with the changes in wind speed ranges from 31.6 to 56.5 TWh yr^{-1} based on the 2019 installed capacity. This estimate explains 22.0%–39.3% of the rapid increase in wind generation CF in China during 2012–2019. The result implies that the site selection of wind farms should consider both current wind situation and future wind speed trends. Further studies are needed to understand the driving factor of wind speed recovery in support of the wind energy industry.

1. Introduction

China is currently the largest CO_2 emitter in the world [1], and has an ambitious plan for emissions to peak by 2030 and achieve carbon neutrality by 2060 [2]. A potentially efficient pathway for curbing CO_2 emissions is to replace fossil fuels with electric power and decrease the carbon intensity of electricity production through renewable energy, e.g. wind power [3]. The cumulative installed wind power capacity in

China has grown exponentially from 5.9 GW in 2007 to 328 GW in 2021 [1, 4, 5]. With over one-third of the world's wind power capacity, China is the world leader in wind power generation [6, 7]. Looking into the future, China's total installed capacity is anticipated to reach 800 GW by 2030 and 3000 GW by 2060 with an additional ∼70 GW installed annually [2].

The efficiency of wind turbines for generating electricity is described as the ratio of the generated power to the rated power, known as the capacity factor (CF) [8, 9]. While the rated power is solely dependent on the number and type of turbines that are installed, the generated power additionally depends on wind farm management (e.g. control of wake effects, maintenance and repair), and wind speed changes [6, 10, 11]. The theoretical maximum wind power is proportional to the cube of wind speed [10]. The amount of those power that can be converted into electricity for any given turbine is further limited by the wind turbine power curve, which can be improved through technology innovation including optimization of blade aerodynamic structure and blade materials [11]. Once turbines have been installed, the power curves are fixed, and the key factor driving power generation is wind speed change [9–11]. Yet, wind speed's impact on the CF for installed wind turbines in China remains unknown, largely owing to (a) debate on how average wind speed has been changing during the past decade when most wind turbines were installed [12–16]; and (b) difficulty in translating the *in-situ* wind records (10 m above ground, daily and discontinuous) into wind power production (i.e. CF) [17–19].

As for wind speed over China, most studies [20–23] report a long-term decreasing trend during 1960–2010, which is consistent with the terrestrial stilling that has been reported globally [12–14]. However, there is no consensus on how wind speed in China has changed since 2010, which marks the beginning of the period when most (more than 85%) wind turbines were installed. Some studies have reported a continuation of the stilling [21–25]; others show a reversal [9, 15]. These differences relate partially to the analysis of *in-situ* records from different subsets of meteorological stations and the application of different quality control criteria [9, 16, 20–23, 25] and lead to the influence of wind speed on wind energy production unknown. For the subsets, recently the HadISD and GSOD datasets have been found to record calm winds inaccurately, particularly for Asian stations including China, producing erroneously high wind speed in recent years [26]. Therefore, the results of Zeng *et al* [9] are likely biased for Asia. It is therefore urgent and necessary to use both China's official dataset and the updated global datasets to determine more accurate wind speeds in China. For the quality control method, Yang *et al* [12] and Tian *et al* [14] also used China's official dataset. Their quality control method necessitated the exclusion of about half of the stations that changed locations over time, potentially biasing the observed wind speed trends, especially for the past decade. Herein, our research aims to clarify the wind speed trend in China using all the four datasets from previous studies and a viable quality control method that preserves more data records without compromising accuracy. Furthermore, we convert the wind speed change to wind energy CF change to quantify the effect of wind speed change on wind energy production.

2. Method

2.1. Wind speed datasets

We used the China Surface Climatic Data Daily Data Set (CSD) (Version 3.0), from the China Meteorological Data Service Center (CMDC; http://data.cma.cn/en/?r=data/; last accessed March 2020). The CSD contains daily mean (average of four observations at 2:00, 8:00, 14:00 and 20:00 now and, three observations at 8:00, 14:00 and 20:00 before installing the automatic recording) data from 699 national-level reference climate stations and basic climate stations in China (not including stations in Hong Kong, Macao and Taiwan) from 1951 until three months before the download time (2020.03) (table S1). Data from 1951 to 2010 were checked for quality both manually and automatically [27]. To get a complete and reliable time series, we only used data from stations for which more than 15 daily observations were available for each month during 1990–2019 [9]. The 15 d criterion is a safety threshold with a sensitivity test, in which we tried 10, 15, 20 and 25 d as thresholds. Benefiting from the integrity of the data, the difference is limited as supplementary figure 1 shows. The distribution of the stations covers all of China's provinces but has a denser coverage in the South East compared with other regions (inset in figure 1). We also applied this quality control method to the other three datasets (see more in supplementary text).

For seasonal analysis, we defined spring as March, April and May, and winter as the following December, January and February, with summer and autumn accordingly defined. For regional analysis, we divided China into six regions based on the partitioned model used in the 2019 Wind Power Industry Report [28], shown in figure 2(a).

2.2. Piecewise regression model

We used the piecewise regression Model 1 mentioned by Toms & Lesperance (2003) to determine turning points and generate the trend lines for the wind speed time series [29]. Model input variables are wind speed time series and the earliest and latest plausible dates for the turning point. We set the turning point to be at least 2 years away from the start and end of the analysis period (1990–2019) to ensure there were

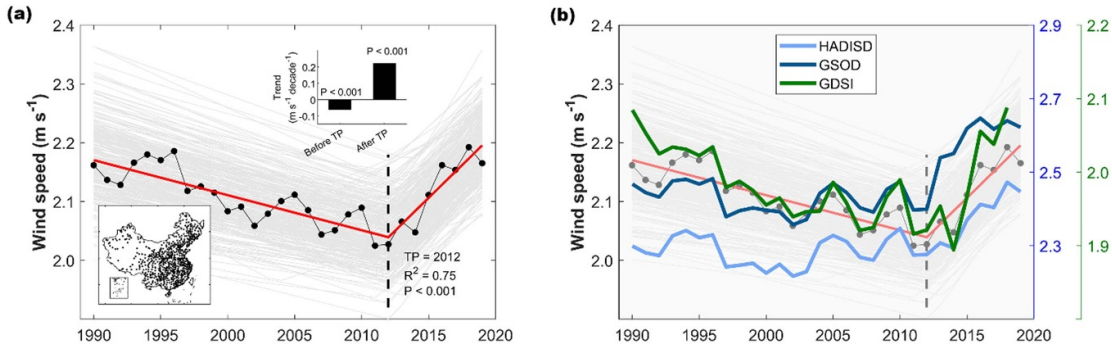

Figure 1. Changes in average terrestrial surface wind speeds for 1990–2019 in China. (a) Each of the 300 grey lines represents a linear fit of a time series formed by a randomly selected subset (40%) of the data. (b) Three other datasets all show a consistent national annual average wind speed recovery in the 2010s. The GSOD (dark blue) and HadISD (light blue) time series correspond to the blue axis on the right.

sufficient data for robust testing. The output from the model is the timing of the turning point, the trends before and after the turning point, the R^2 for the piecewise regression, the P value for the timing of the turning point, the first and the second partial fit and the complete model fit. The calculation of the P value is based on the t-test null hypothesis: the trend difference before and after the tested point is 0.

2.3. CF calculation

We refer to three types CFs: (a) real CF (CF_{real}, orange line shown in figure 3) is based on the data statistics; (b) calculated raw CF (CF_{raw}, left axis in figure 4) is our raw calculation from wind speed; (c) calibrated CF (CF_{cali}, right axis in figure 4) is CF_{raw} calibrated by CF_{real} as shown in equation (4).

Both CF_{real} and CF_{raw} are calculated from the following equation:

$$CF = \frac{P_{real}}{P_{rated}}. \quad (1)$$

For national CF_{real}, the rated power (P_{rated}) is the national installed wind capacity (unit: GW) and the real power (P_{real}) is the annual net wind power generation (unit: GWh) in China taken from the U.S. Energy Information Administration (www.eia.gov/opendata/) divided by 8760 h (hours in a year). The provincial CF_{real}s come from the annual wind power grid-connected operation statistics reported by National Energy Administration of China (www.nea.gov.cn/).

National and provincial CF_{raw}s were calculated from monthly average wind speeds as follows: (a) we converted monthly wind speeds data into hourly data; (b) we used a power curve to convert wind speed to output power, allowing the calculation of the CF; (c) we use Thiessen Polygon to calculate the national and provincial average CF_{raw}s. For the first step, we used 33 stations with hourly observations in the corrected HadISD dataset as reference stations (the distribution of the reference stations is shown in figure S2a). The hourly wind speed distribution for a given month was assumed to follow the Weibull distribution associated with the nearest reference station (figure S3, equation (2)) [30, 31]:

$$f(x;\lambda,k) = \begin{cases} \frac{k}{\lambda}\left(\frac{x}{\lambda}\right)^{k-1} e^{-(x/\lambda)^k}, & x \geqslant 0 \\ 0, & x < 0 \end{cases} \quad (2)$$

where λ and k are the parameters that determine the distribution using the function called 'wblfit' in MATLAB. A detailed description of this method is provided by Sweerts *et al* [32].

For the second step, we used an exponential wind profile power law relationship [14] to convert the observed wind speeds (u at height $z_s = 10$ m) to wind speeds at the hub height of the wind turbines (u_{tb} at hub height $z_{tb} = 85$ m):

$$u_{tb} = u\left(\frac{z_{tb}}{z_s}\right)^{\alpha} \quad (3)$$

where α is estimated using equation (3) with the hourly 10 m and 100 m wind speed in the ERA5 reanalysis: we determined the α for each location as the 2017–2019 average and the result is shown in supplementary figure 4. We then use the power curve (figure S5) to convert wind speed to output power. We chose the power curve from the Goldwind model GW 121/2500, with 2.5 MW rated power, 85 m hub height and 121 m rotor diameter. The cut-in and cut-out wind speeds for this turbine are 3 m s^{-1} and 22 m s^{-1} respectively (figure S5) [33]. The GW 121/2500 turbine is selected as Goldwind has the largest wind power market share in China and this turbine is one of the most commonly installed [34]. With the energy production, we can calculate the CF_{raw}s according to equation (1).

For the third step, we calculate the areas of the polygons in the Thiessen Polygon map (figure S6) determined for the stations in CSD dataset. The calculated national and provincial CF_{raw}s are reported as the area weighted average values for these polygons.

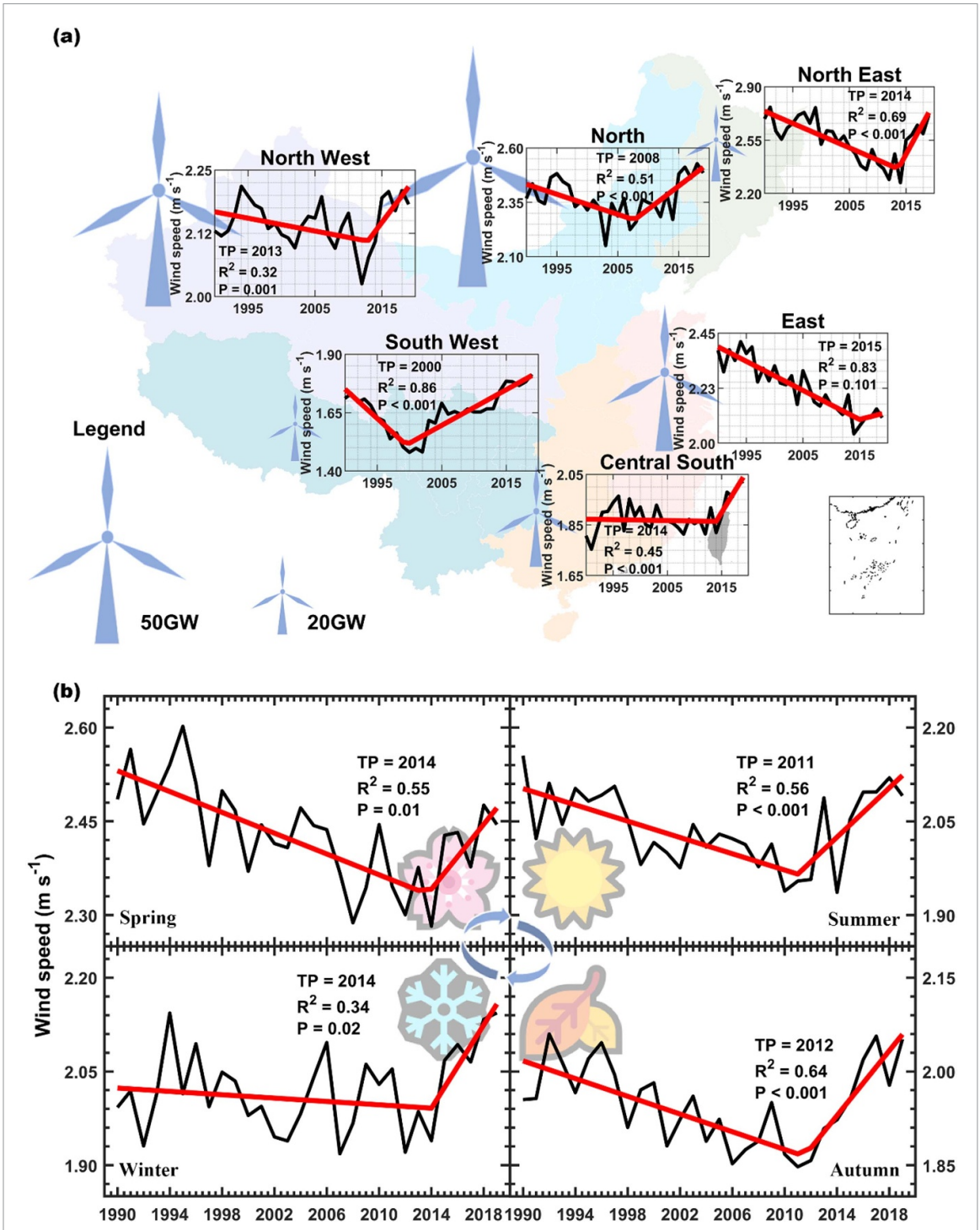

Figure 2. Spatiotemporal analysis of wind speed trends. (a) Regional wind speed trends and installed capacity. The text insets indicate the timing of the detected turning point, R^2 for the fitted model, and the significance of the turning point timing. (b) Wind speed trends in different northern hemisphere seasons.

The calculated CF_{raw}s are lower than CF_{real}s because we use weighted area rather than actual wind farm distribution. In reality, wind farms are only located in areas with good wind resources, and the type of wind turbine was always carefully selected to match local weather conditions. Using CF_{raw} will underestimate the contribution of the average wind speed change to the CF_{real} change. Therefore, when calculating the gain driven by wind speed recovery, we first converted CF_{raw} into real magnitude. The multiplier ($\beta = 1.78$) was defined as the ratio of CF_{real} (0.225) and CF_{raw} (0.126) in 2019 (our turbine data was based on the technology in 2019). This way, the effect of technology improvement is controlled to be the same. The CF_{cali} was calculated as

$$CF_{cali} = \beta \cdot CF_{raw} \quad (4)$$

where β is only suitable for a national value of 2.5 MW turbine and should not be used for provincial values nor for other turbines.

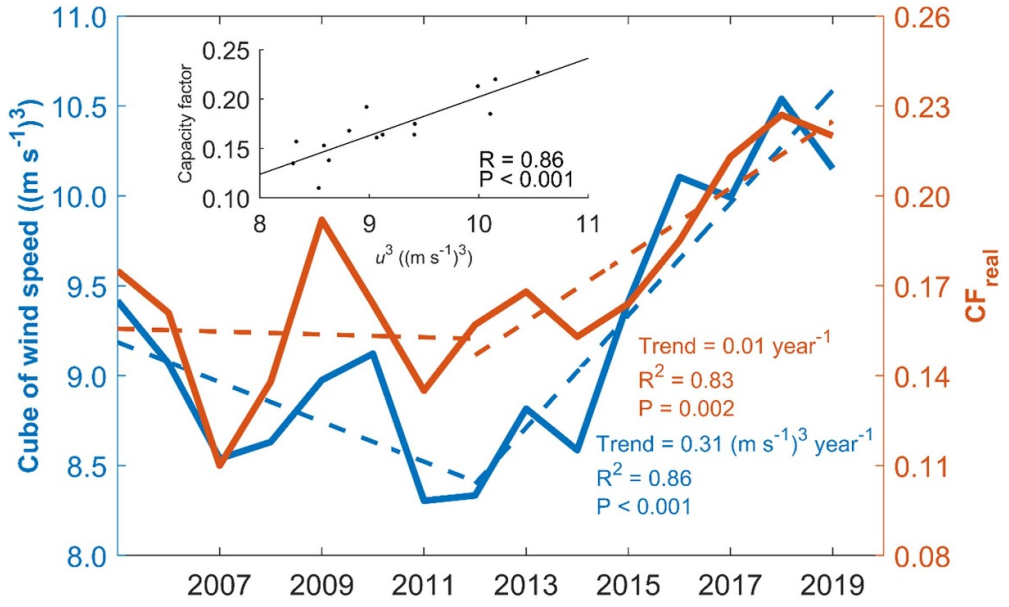

Figure 3. The wind power CF for China during 2005–2019 depends on the cube of the wind speed. The blue line (left *y*-axis) is the cube of wind speed and the orange line (right *y*-axis) is CF_{real}. The separation in 2012 reflects the detected turning point in wind speed. The inset figure shows the significant relationship between the capacity factor and the cube of the wind speed.

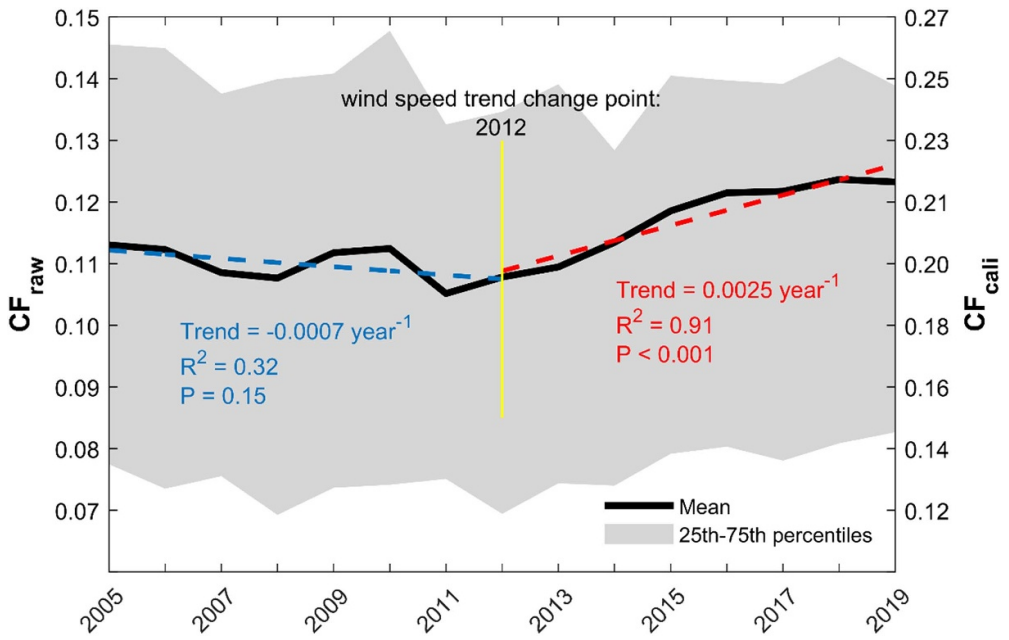

Figure 4. Estimation of the change in the capacity factor driven by wind speed. The black line is the national mean CF_{raw} (left axis) and CF_{cali} (right axis). Blue and red dashed lines are the linear fits of CF_{raw}/CF_{cali} before and after wind speed change point in 2012 (yellow line) accordingly.

3. Results

3.1. The recovery of wind speed in China since 2012

Our results show that after several decades of decreasing trend, the wind speed in China has significantly increased since 2012 ($P < 0.001$, figure 1(a)). The R^2 of the piecewise regression model is 0.75 with a wind speed decreasing trend of -0.060 m s^{-1} $decade^{-1}$ during 1990–2012 ($P < 0.001$, inset of figure 1(a)). Following the reversal, the increase in wind speed has a four-fold higher magnitude during the rest of the decade (0.223 m s^{-1} $decade^{-1}$; $P < 0.001$, inset of figure 1(a)). Specifically, 59% of the stations show increasing trends and 41% of them are significant ($P < 0.05$; figure S7). To ensure that the turning point is not caused by strong variations in wind speed at individual stations, we also performed piecewise linear regression on 300 data subsets, each containing 268 stations (40% of the total) that were selected

Table 1. Wind power production range (Table_FootNote [a]) considering different wind speed levels and different capacities (TWh yr^{-1}) based on the 2019 technology level.

Average wind speed	Average CF	Capacity		
		210.1 GW (2019)	800 GW (2030)	3000 GW (2060)
2.20 m s^{-1} (2019)	0.1260–0.2249	231.8–413.8	883.0–1576.1	3311.3–5910.3
2.71 m s^{-1} (historical highest)	0.1713–0.3058	315.2–562.6	1200.5–2142.7	4501.8–8035.2
2.04 m s^{-1} (historical lowest)	0.1088–0.1942	200.2–357.3	762.5–1360.9	2859.3–5103.5

[a] The first and second values are (or base on) CF_{raw} and CF_{cali} accordingly.

randomly from the whole dataset (grey lines in figure 1(a)). All the subsamples show significant turning points with $P < 0.001$; and R^2 exceeds 0.55 for 96% of the linear regression models. The 95% confidence interval for the turning point location is also 2012 for the subsamples.

To test the robustness of the reversal of wind speed trend in China, we repeated our analysis using other station-based and quality-controlled datasets, including the Global Surface Summary of the Day from the U.S. National Oceanic and Atmospheric Administration (GSOD), the Hadley Integrated Surface Database from the U.K. Met Office Hadley Centre (HadISD), and a private dataset from the Geographic Data Sharing Infrastructure of Peking University (GDSI). All the datasets show a rapid increase in the 2010s (figure 1(b)), which again is the period when installed wind capacity in China became prominent [1, 4, 5].

3.2. Spatiotemporal variability of the wind speed recovery

The wind speed recovery varies significantly for different regions of the country (figure 2(a)). The recovery started in the South West in 2000, increasing twice in 2003 and 2014. Later it gradually spread among regions, first to the North in 2008, then to the North West in 2013, the North East in 2014, the Central South in 2014, and finally to the East in 2015. The time series of wind speed trends in the North East, Central South and the North, have similar upward changes following distinct turning points centering around 2010 (the trends change by more than 0.3 m s^{-1} $decade^{-1}$, $R^2 > 0.45$, $P < 0.001$). The wind speed in the East decreased continuously until 2015 without a significant turning point ($P = 0.101$). The wind speed in the North West fluctuates greatly and the piecewise regression model has the lowest R^2 of 0.32.

As for seasonal variability, the most significant reversal occurred in autumn ($R^2 = 0.64$, $P < 0.001$). Autumn wind speeds decreased in 1990–2011 (-0.071 m s^{-1} $decade^{-1}$) then increased substantially in 2011–2019 (0.260 m s^{-1} $decade^{-1}$). Winter wind speeds did not decrease much during 1990–2012 (-0.013 m s^{-1} $decade^{-1}$) but increased rapidly after 2012 (0.333 m s^{-1} $decade^{-1}$). The spatiotemporal variability in the wind speed recovery (figure 2 and S8) indicates that a reliable estimation of wind power gain requires fine-scale analysis both spatially and temporally (e.g. by hourly and for smaller area).

3.3. Relationship between capacity factor increase and wind speed recovery

We found that the overall CF in China (CF_{real}) is highly correlated with the cube of wind speed ($R = 0.86$, $P < 0.001$; figure 3), demonstrating the non-negligible role of wind speed in the interannual variability of CF for wind generation. Especially, during 2012–2019, the cube of wind speed in China increased significantly by 26% ($R^2 = 0.86$, $P < 0.001$), and the CF increased by 56% ($R^2 = 0.83$, $P = 0.002$), indicating that the recent recovery of wind speed is likely improving the efficiency of installed wind turbines. For installed wind turbines with fixed rated power, increasing wind speeds generate more wind power, increasing the CF.

3.4. Estimation of capacity factor increase boosted by wind speed recovery

To estimate the wind power gain and the CF growth solely driven by the increase in average wind speed, we calculated the CF_{raw} with all other variables controlled (e.g. turbine technology improvement, wind farm expansion; see detail in *Methods*). We found that CF_{raw} increased by 17% (from 0.1088 in 2012 to 0.1260 in 2019), accounting for 22.0% of the CF_{real} increase (from 0.1468 in 2012 to 0.2249 in 2019). After calibration, CF_{cali} increase equals 39.3% of the CF_{real} increase. The corresponding increase in electricity generation is 31.65–56.49 TWh yr^{-1} (the lower and upper boundary are based on CF_{raw} and CF_{cali} accordingly; the following is the same) based on the total installed capacity in 2019 (210.05 GW, table 1). Both the upper and lower quartile in figure 4, corresponding to the provinces with abundant and limited wind resources respectively, experienced a slightly decreasing trend followed by a recovery. However, this assessment is not robust because the time series are short. At the province level, although the records are available only since 2013, we found that the trend of our calculated CF is consistent with values reported in most provinces (figures 5, 6 and S9). Considering that our calculation only uses the wind speed data and a single turbine type, the consistency provided additional convincing evidence that wind speed is a key factor attributing to the change in CF. Furthermore,

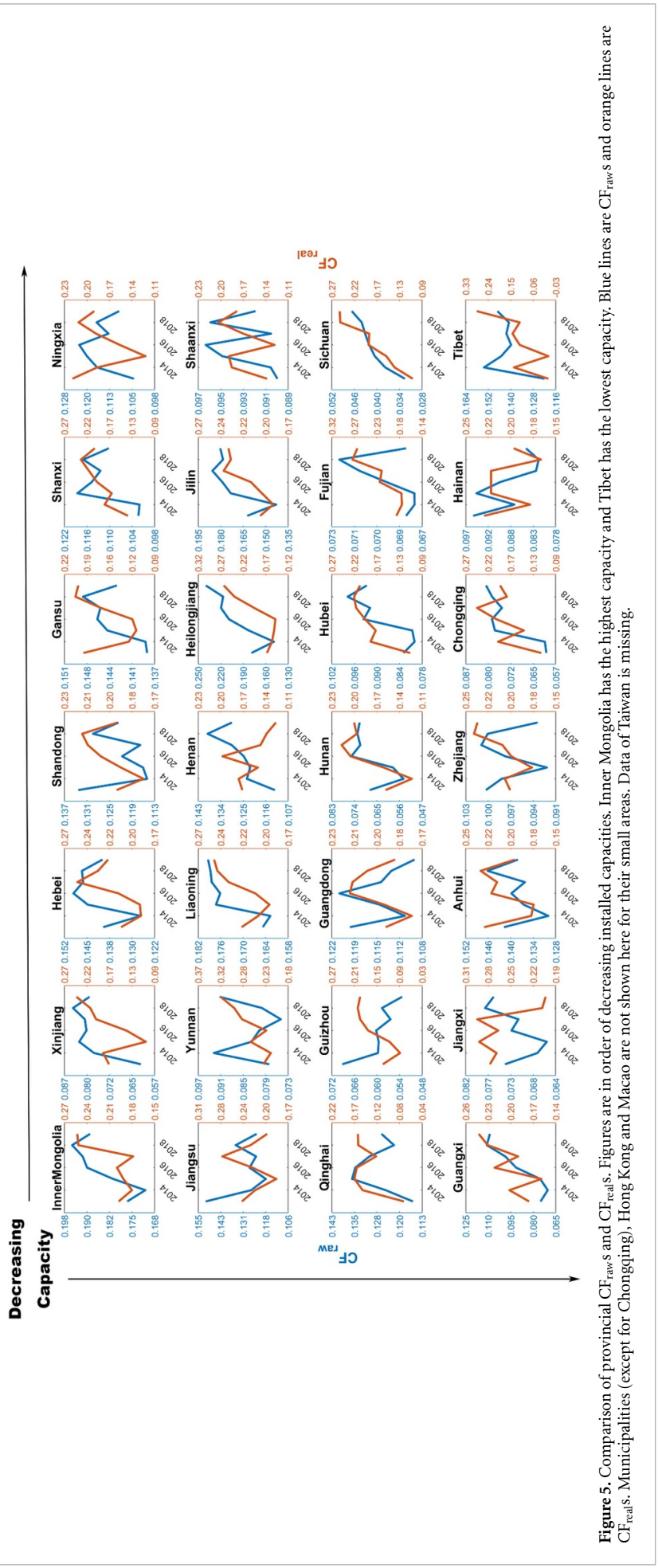

Figure 5. Comparison of provincial CF_{raw}s and CF_{real}s. Figures are in order of decreasing installed capacities. Inner Mongolia has the highest capacity and Tibet has the lowest capacity. Blue lines are CF_{raw}s and orange lines are CF_{real}s. Municipalities (except for Chongqing), Hong Kong and Macao are not shown here for their small areas. Data of Taiwan is missing.

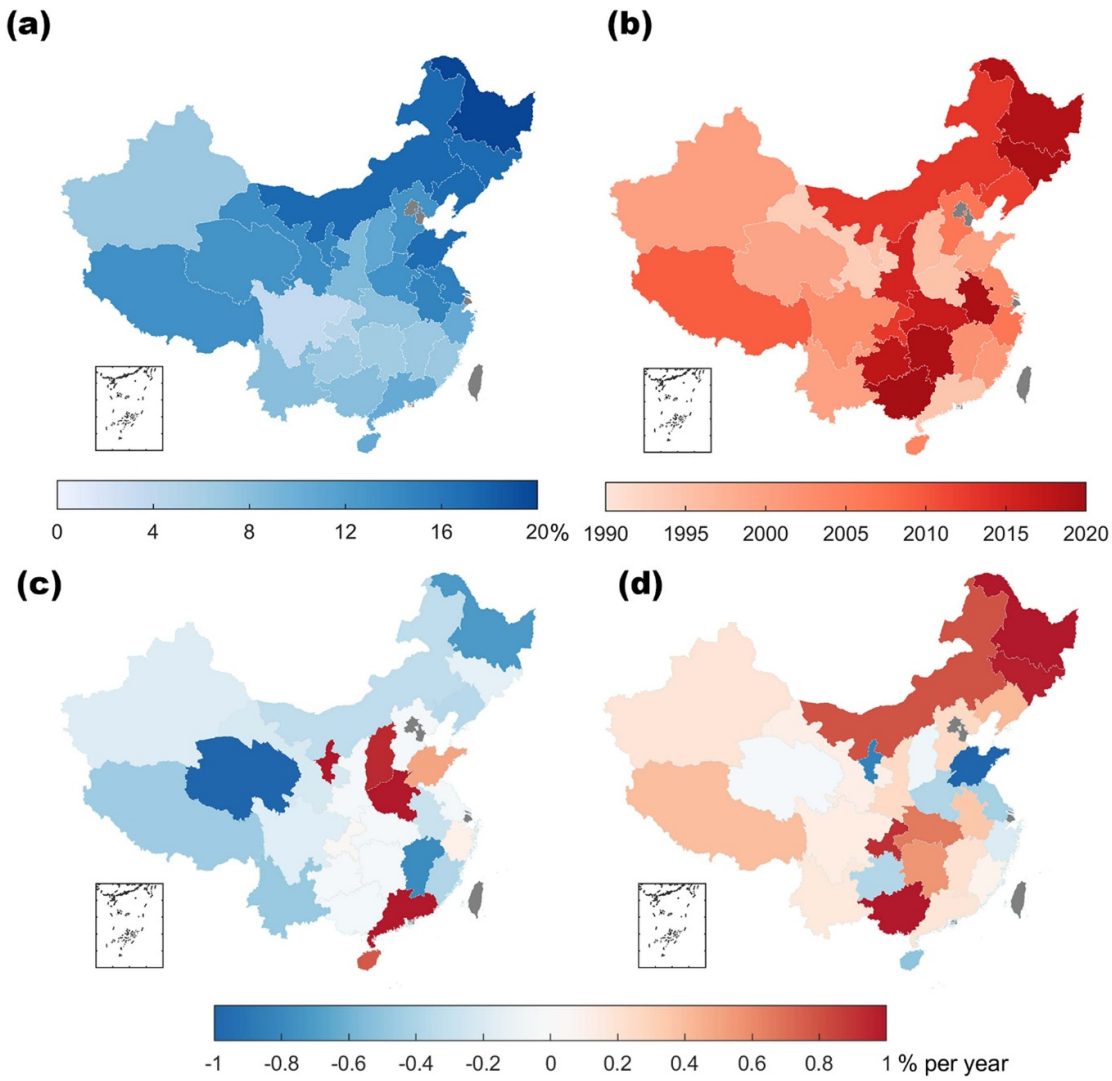

Figure 6. Provincial average CF_{raw} trends and turning points. (a) Average provincial CF_{raw}s for 1990–2019. (b) Turning points of provincial CF_{raw}s. (c) CF_{raw} trends before the turning points. (d) CF_{raw} trends after the turning points. Grey area (e.g. Taiwan) means no data.

we also tried other wind turbine types (table S2) and found that the trend changes were robust regardless of which turbine model was selected (figure 7).

With increasing installed capacity, the gain of wind power brought by the recovery of wind speed is potentially large. We set three scenarios to quantify the wind energy production potential. In the first scenario, which holds wind speed at the current level (2.20 m s^{-1} in 2019), the wind energy production will be 3311.3–5910.3 TWh yr^{-1} in 2060, equal to 40%–71% of the electricity consumption of China in 2021 (8312.8 TWh yr^{-1} [35]). The second scenario considered that wind speed might be influenced by decadal periodicity in ocean-atmosphere circulation [36] and potentially return to its historically highest level in 1969 (2.71 m s^{-1}, figure S10). For this hypothetical scenario, the wind power production would be 4501.8–8035.2 TWh yr^{-1} in 2060, equaling the production of 40–72 Three Gorges dams (111.8 TWh in 2019 [35]). The third scenario considered wind speed would decrease as *IPCC* predicted [37]. We took the historically lowest level (2.04 m s^{-1}) in 2012 as the potential wind speed. In this case, the 3000 GW capacity will only generate total electricity of 2859.3–5103.5 TWh yr^{-1} (figure 7, table 1).

4. Discussion

All four data series mentioned above show upward trends in the 2010s (figure 1(b)). However, the turning points visible in the CSD and GDSI datasets from CMDC occur around 2010, which is about one decade later than those seen in the GSOD and HadISD datasets (around 2000). This dissimilarity may stem from differences in the number and distribution of stations (table S1, figure S1). However, we also found that some stations with the same station ID in the HadISD and CSD datasets have time series abruptly become dissimilar following a long-term consistency. This discrepancy may be caused by: (a) stations being

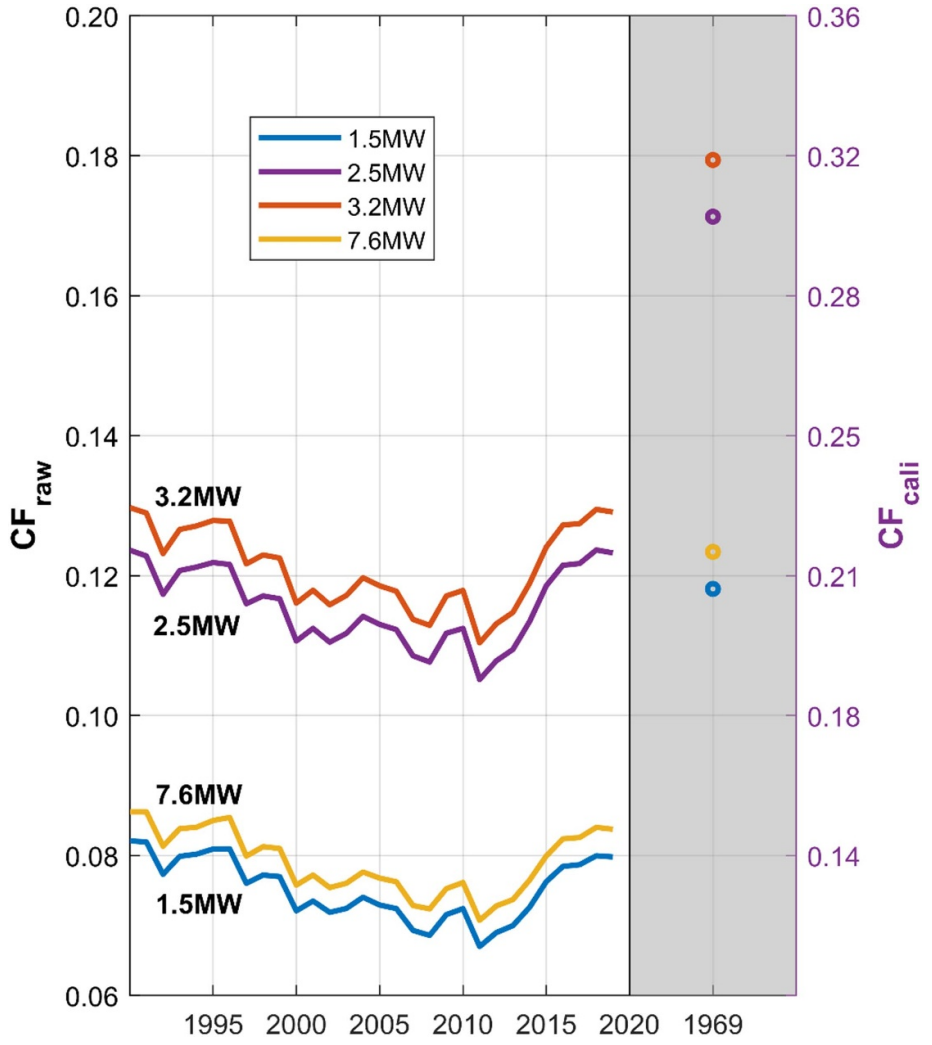

Figure 7. Comparison of CF_{raw}s for different turbines. Dots in the grey area shows the CF_{raw}s of the historical highest wind speed in 1969. The right *y*-axis (purple color) is CF_{cali} only applies to 2.5 MW turbine (purple color).

merged in HadISD [38] and (b) station relocation which has been processed with a spatial consistency check and corrected by CSD [27], but not by HadISD. Through the comparison of some overlapping stations in HadISD and CSD, the CSD data tend to have fewer such abrupt changes (figure S11).

The reason for the wind recovery remains unclear, leading to uncertainty about the future wind speed trend and wind power potential [37]. The driver of long-term wind speed decrease in China has two facets: (a) reduction of driving force associated with the change of large-scale atmospheric circulation [9, 25, 39] and (b) increase in resistance associated with land use/land cover change [13, 21, 40, 41]. Considering that the land change trend is unlikely to reverse suddenly in 2012, the increasing wind speed is potentially a result of changed atmospheric circulation change [9]. Ongoing research is exploring these relationships and the associated physical processes. For example, the West Pacific Index (WPI) shows a more positive pattern during the period of wind speed decreases and a more negative pattern when wind speed recovers [42]. Negative phases of WPI mean more Western North Pacific tropical cyclones move into southern China and bring wind [43]. The increasing negative phases of Southern Oscillation Index (SOI) during 1975–2000 means colder sea water, smaller land-ocean air pressure gradient and weaker winter winds in China [16, 44]. While the recovery of SOI positive phases since 2000 is followed by the reversal of wind speed. However, the relationship between the East Asian winter monsoon and SOI is unstable [45]. By now, no model fully reproduces the wind speed historical trends [37]. Additional studies in this field are needed considering the rapid growth in installed wind power globally.

Our analyses are based on a singular 2.5 MW wind turbine model. To address the uncertainty, we also calculated the CFs of turbines with rated capacities of 1.5 MW, 3.2 MW and 7.6 MW. The result shows that the 3.2 MW and 2.5 MW wind turbine models have much higher CFs than the 1.5 MW and 7.6 MW models for all the three wind speed scenarios (figure 7). Considering that 3.2 MW turbines

can produce more electricity than 2.5 MW turbines for the same CF, this model is arguably an ideal choice for the observed/predicted wind trends instead of larger capacity of a 7.6 MW turbine. Choosing appropriately sized turbines based on wind situation can help narrow the CF gap between China and the United States [8, 9, 46].

5. Conclusion

Our analysis shows that following decades of decreasing wind speeds, wind speeds have recovered in most places in China in the 2010s. This reversal in wind speed trend has significant implications for wind power production. We used an innovative method to calculate the wind speed-driven CF change and found that this recovery has increased the CF for wind generation in China by 17%, explaining almost 22.0%–39.3% of the reported increases in the CF over 2012–2019. This change in wind speed allows wind farms to be more efficient sources of electricity generation, and therefore, supports the role of wind energy development to help replace fossil fuels in the future. However, the underlying cause of wind speed change remains unclear, lending uncertainty to the prediction of future wind speeds. To explore this uncertainty, we used three possible scenarios related to wind speed changes (reduction, increase and stay). But further research is still required to make a more informed conclusion. An improved understanding of the drivers of changes in wind speed can provide a basis for improved regulation of wind farms siting, turbine selection and management.

Data availability statement

The data that support the findings of this study are available upon reasonable request from the authors.

Acknowledgments

This study was supported by the National Natural Science Foundation of China (Grant No. 42071022) and the start-up fund provided by Southern University of Science and Technology (No. 29/Y01296122). C A M was supported by the IBER-STILLING Project RTI2018-095749-A-100 (MCIU/AEI/FEDER,UE), the VENTS Project AICO/2021/023 (GVA), the 2021 Leonardo Grant for Researchers and Cultural Creators from the BBVA Foundation, and the CSIC Interdisciplinary Thematic Platform PTI-CLIMA.

Thank Adrian Chappell for discussions on earlier version of the manuscript

Author contributions

Zhenzhong Zeng: Conceptualization, Methodology Yi Liu: Methodology, Software, Data Curation, Writing—Original Draft All other authors: Writing—Review & Editing

Conflict of interest

The authors declare no competing financial interests.

ORCID iDs

Yi Liu https://orcid.org/0000-0002-5515-8804
Sonia Jerez https://orcid.org/0000-0002-2153-1658
Deliang Chen https://orcid.org/0000-0003-0288-5618
Xinrong Yang https://orcid.org/0000-0001-9469-9884
Feng Zhou https://orcid.org/0000-0001-6122-0611
Junguo Liu https://orcid.org/0000-0002-5745-6311

References

[1] Looney B 2020 BP statistical review of world energy (The British Petroleum Company)
[2] Global Wind Energy Council 2020 Beijing declaration on wind energy (available at: https://gwec.net/wp-content/uploads/2020/11/Beijing-Declaration-EN.pdf)
[3] Masson-Delmotte V *et al* 2018 Global warming of 1.5 C, an IPCC special report on the impacts of global warming (Intergovernmental Panel on Climate Change)
[4] U.S. Energy Information Administration 2020 Wind electricity installed capacity (available at: https://www.eia.gov/international/overview/country/CHN)
[5] International Renewable Energy Agency 2019 Future of wind: deployment, investment, technology, grid integration and socio-economic aspects
[6] Lewis J I 2016 Wind energy in China: getting more from wind farms *Nat. Energy* **1** 16076
[7] McElroy M B, Lu X, Nielsen C P and Wang Y J S 2009 Potential for wind-generated electricity in China *Science* **325** 1378–80
[8] Huenteler J, Tang T, Chan G and Anadon L 2018 Why is China's wind power generation not living up to its potential? *Environ. Res. Lett.* **13** 044001
[9] Zeng Z *et al* 2019 A reversal in global terrestrial stilling and its implications for wind energy production *Nat. Clim. Chang* **9** 979–85
[10] Lu X, McElroy M B and Kiviluoma J 2009 Global potential for wind-generated electricity *Proc. Natl Acad. Sci. USA* **106** 10933–8
[11] Veers P *et al* 2019 Grand challenges in the science of wind energy *Science* **366** 2027
[12] Yang Q, Li M, Zu Z and Ma Z 2021 Has the stilling of the surface wind speed ended in China? *Sci. China Earth Sci.* **64** 1036–49
[13] Vautard R, Cattiaux J, Yiou P, Tépaut J N and Ciais P 2010 Northern Hemisphere atmospheric stilling partly attributed to an increase in surface roughness *Nat. Geosci.* **3** 756–61
[14] Tian Q, Huang G, Hu K and Niyogi D 2019 Observed and global climate model based changes in wind power potential over the Northern Hemisphere during 1979–2016 *Energy* **167** 1224–35
[15] China Meteorological Administration 2020 *Blue Book on Climate Change in China 2020* (Beijing: Science Press)

[16] Zhang G et al 2020 Variability of daily maximum wind speed across China, 1975–2016: an examination of likely causes J. Clim. 33 2793–816
[17] Barthelmie R J and Jensen L E 2010 Evaluation of wind farm efficiency and wind turbine wakes at the Nysted offshore wind farm Wind Energy 13 573–86
[18] Chang T J, Wu Y T, Hsu H Y, Chu C R and Liao C M 2003 Assessment of wind characteristics and wind turbine characteristics in Taiwan Renew. Energy 28 851–71
[19] Al-Yahyai S, Gholamreza R and Abdol Azim G 2016 Wind resource assessment over Iran using weather station data Int. J. Sustain. Energy 35 230–43
[20] Chen L, Li D and Pryor S C 2013 Wind speed trends over China: quantifying the magnitude and assessing causality Int. J. Climatol. 33 2579–90
[21] Mcvicar T R et al 2012 Less bluster ahead? Ecohydrological implications of global trends of terrestrial near surface wind speeds Ecohydrology 5 381–8
[22] Miao H et al 2020 Evaluation of Northern Hemisphere surface wind speed and wind power density in multiple reanalysis datasets Energy 200 117382
[23] Wang K, Zhang Z, Chen D, Li J and Dickinson R 2019 Increase in surface friction dominates the observed surface wind speed decline during 1973–2014 in the Northern Hemisphere lands J. Clim. 32 7421–35
[24] Zhang X, Shen B and Huang L 2020 Spatiotemporal variation of near surface wind speed over China based on ITPCAS reanalyzed dataset Arid Zone Res. 37 1–9
[25] Ding Y, Li X and Li Q 2020 Advances of surface wind speed changes over China under global warming J. Appl. Meteorol. Sci. 31 1–12
[26] Dunn R J H, Azorin-Molina C, Menne M J, Zeng Z, Casey N W and Shen C 2022 Reduction in reversal of global stilling arising from correction to encoding of calm periods Environ. Res. Commun. 4 061003
[27] China Meteorological Administration 2017 Meteorological data set description document (available at: https://data.tpdc.ac.cn/zh-hans/data/52c77e9c-df4a-4e27-8e97-d363fdfce10a/)
[28] Beijixing 2020 2019 wind power industry report
[29] Toms J D and Lesperance M L 2003 Piecewise regression: a Tool for identifying ecological thresholds Ecology 84 2034–41
[30] Seguro J V and Lambert T W 2000 Modern estimation of the parameters of the weibull wind speed distribution for wind energy analysis J. Wind Eng. Ind. Aerodyn. 85 75–84
[31] Akdağ S A and Dinler A 2009 A new method to estimate weibull parameters for wind energy applications Energy Convers. Manage. 50 1761–6
[32] Sweerts B et al 2019 Estimation of losses in solar energy production from air pollution in China since 1960 using surface radiation data Nat. Energy 4 657–63
[33] Goldwind 2019 2.5WM PMDD Wind Turbine (available at: https://newgoldwind.coppabellawindfarm.com/wp-content/uploads/2019/12/GW2.5-Product-Brochure-Web.pdf.)
[34] Chinese Wind Energy Association 2019 China wind power industry map 2018 (available at: http://cwea.org.cn/industry_data_2018.html)
[35] National Energy Administration of China 2020 Wind power grid operation in 2019 Goverment Data Report (available at: http://www.nea.gov.cn/2020-02/28/c_138827910.html)
[36] Zha J, Shen C, Zhao D, Wu J and Fan W 2021 Slowdown and reversal of terrestrial near-surface wind speed and its future changes over eastern China Environ. Res. Lett. 16 034028
[37] IPCC 2021 Climate change 2021: the physical science basis Contribution of Working Group I to the Sixth Assessment Report of the Intergovernmental Panel on Climate Change (Cambridge: Cambridge University Press)
[38] Dunn R J H, Willett K M, Morice C P and Parker D E 2014 Pairwise homogeneity assessment of HadISD Clim. Past 10 1501–22
[39] Lu X, McElroy M B, Chen X and Kang C J 2014 Opportunity for offshore wind to reduce future demand for coal-fired power plants in China with consequent savings in emissions of CO_2 Environ. Sci. Technol. Lett. 48 14764–71
[40] Wu J, Zha J, Zhao D and Yang Q 2018 Changes of wind speed at different heights over eastern China during 1980–2011 Int. J. Climatol. 38 4476–95
[41] Zha J, Zhao D, Wu J and Zhang P 2019 Numerical simulation of the effects of land use and cover change on the near-surface wind speed over Eastern China Clim. Dyn. 53 1783–803
[42] NOAA 2012 West pacific pattern (positive phase): historical time series (available at: www.cpc.ncep.noaa.gov/data/teledoc/wp_ts.shtml) (Accessed 15 September 2022)
[43] Choi K S and Moon I J 2012 Influence of the Western Pacific teleconnection pattern on Western North Pacific tropical cyclone activity Dyn. Atmos. Oceans. 57 1–16
[44] NOAA 2022 Southern oscillation index (SOI) (available at: www.ncei.noaa.gov/access/monitoring/enso/soi) (Accessed 15 September 2022)
[45] Wang H, He S and Liu J 2013 Present and future relationship between the East Asian winter monsoon and ENSO: results of CMIP5 J. Geophys. Res. Oceans 118 5222–37
[46] Lu X et al 2016 Challenges faced by China compared with the US in developing wind power Nat. Energy 1 1–6